Investigation of the Al-rich Al-Cu-Mg Alloy System

Nishimura, Hideo

Investigation of the Al-rich Al-Cu-Mg Alloy System.

By Hideo Nishimura.

Introduction.

For the fundamental investigation of such high tensile Aluminium alloys as Duralumin and Superduralumin, it is necessary to ascertain the equilibrium diagram of the Al-rich Al-Cu-Mg system. This system, however, has not been investigated systematically since the publication of Vogel[1]. Even though his diagram is not complete, no attention has been paid to this Al-Cu-Mg system. The diagram in solid equilibrium state given by Gayler[2] is also discussed from the stand point of Vogel's diagram. Fuss cited them in his recent edition[3].

But these diagrams are too incomplete to explain the ageing phenomena of Al alloys for the following reason.

Such Aluminium alloys containing Cu and Mg as Duralumin and 24S-type Super-duralumin show a marked hardening when they are quenched from temperatures as high as 500°C and aged at room temperature. It has been considered hitherto that this age-hardening is due to the marked decrease of solid solubility of $CuAl_2$ or Mg_2Si in Aluminium from higher temperatures to lower. However this theory and also the diagrams of Al-Cu-Mg given by Vogel and other authors do not explain why the Aluminium alloys containing simultaneously Cu and Mg age at room temperature and the alloys containing either Cu or Mg_2Si do not harden at room temperature, but show considerable hardening by tempering at 150°–170°C.

The author considered that the equilibrium diagram Al-Cu-Mg must be investigeted to ascertain the relation between these ageing phenomena. For this purpose, this investigation has been carried out, and in consequence, we were able explain the reason why duralumin age-hardens at room temperature. The equilibrium diagram of the Al-rich Al-Cu-Mg Alloy System is published in this paper.

Principle of Investigation.

To determine this diagram, it is necessary to ascertain the binary systems Al-Cu and Al-Mg. The system Al-Cu, however, has been thoroughly investigated by C. Hisatsune[4] in my laboratory and the diagram Al-Mg has been also published by many authors, such as Hanson and Gayler, Kawakami[5], Hamazumi[6], Köster and Dullenkopp[7], etc. Even if some differences in the latter system are recognized in the results of their investigations, we had no need to enter into a discussion of the differences.

In the present investigation, ternary alloys corresponding to the sections containing constant contents of Al or passing the Al-axis were prepared, and their cooling and heating curves were obtained by thermal analyses. Thus the liquidus and solidus surfaces or the invariant reactions in this system have been determined. The solid solubilities of Cu and Mg in Al were determined from the measurement of thermal expansion. From the results of these experiments the general equilibrium diagram of this system was obtained in the range of 50% of Cu and 30% of Mg.

Method of Investigation.

Preparation of Specimens. Specimens were prepared of Aluminium 99.8% pure, Magnesium 99.9% pure and electrolytic copper. They were melted and cast in a chilled mould, and after analysis, they were employed in the experiments.

Fig. 1.

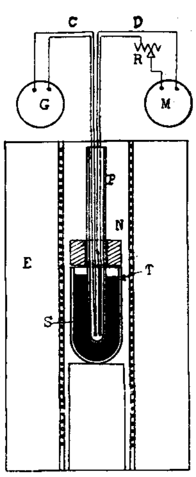

Thermal analysis. Cooling curves from liquid were obtained by the arrangement as shown in Fig. 1. In the figure, E is a nichrome-wound electric tube furnace in which a Tammann tube T is set, and the specimen S in the Tamman tube is heated in the furnace. A porcelain tube P is inserted in the hole of the specimen, and a porcelain cylinder N as neutral body is put through the porcelain tube on the Tammann tube.

Thermo-couple C and differential couple D are inserted together in the porcelain tube P, the former being connected to the pyrometer-galvanometer and the latter to the Leeds and Northrup Mirror-galvanometer. Thus either the temperature or the deflection of the

1) Z. anorg. Chem. 75 (1912) 41, 107 (1919) 265.
2) J. Inst. Metals, 29 (1923) 507.
3) Metallographie des Aluminium- und Seine Legierungen.
4) Tetsuto-Hagane, 21 (1935) 726.
5) Kinzoku no-Kenkyu, 10 (1933) 535.
6) Tetsu-to-Hagane, 22 (1936) 258.
7) Z. Metallk. 28 (1936) 309.

Fig. 2.
Cooling curves

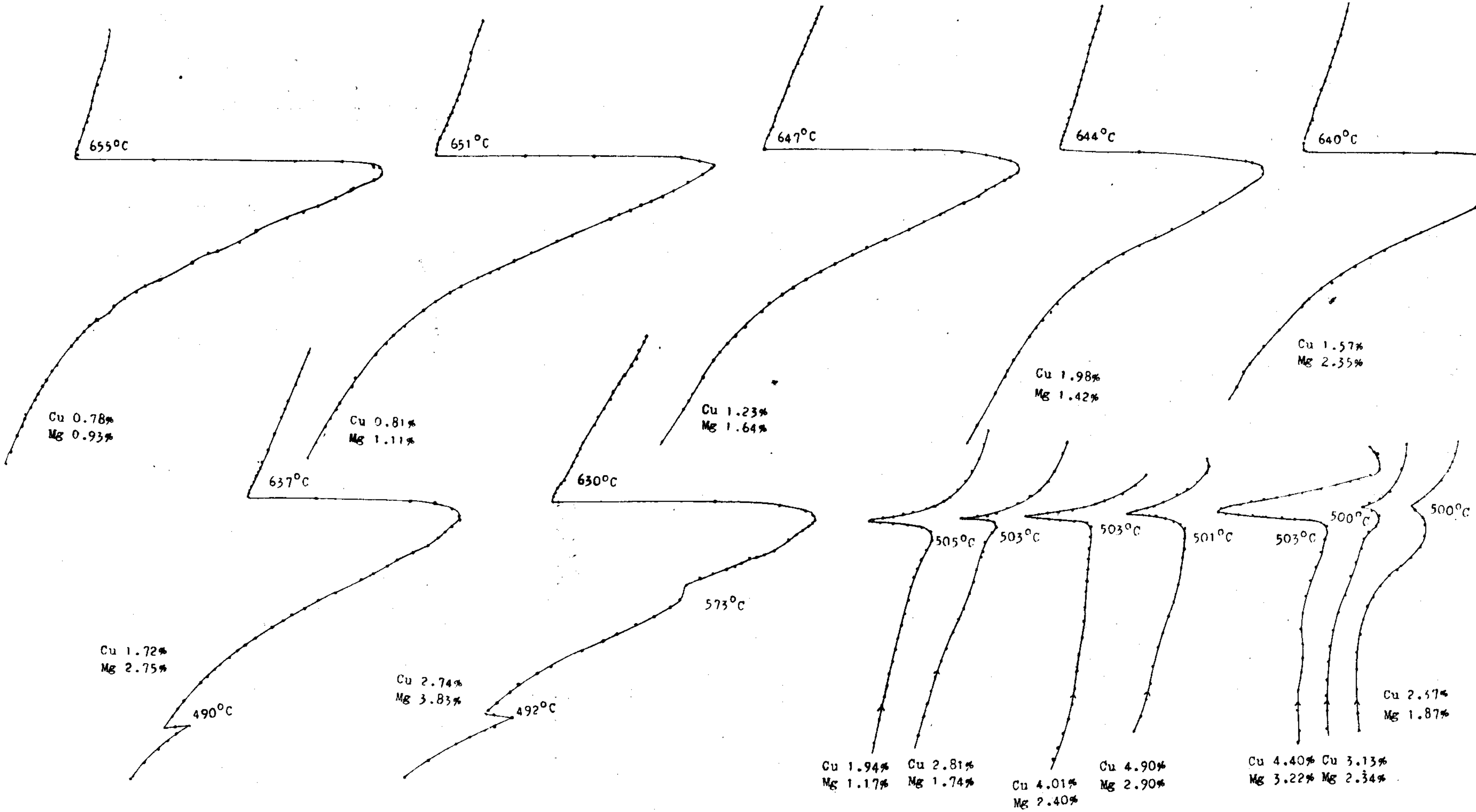

Heating curves

mirror was read on cooling by the pyrometer-galvanometer and the telescope and scale respectively. In this experiment the Mg-rich alloys were protected from oxidation by a flux consisting of 25% Potassium bichromate and 75% Sodium bichromate with the addition of 3% Potassium chromate. Some examples of cooling curves are shown in Fig 2.

To determine the solidus point, thermal analysis was carried out on the annealed specimen as shown in Fig. 3, i.e. the hole, as shown in the Fig., is bored in an Al cylinder and specimen *S* is inserted in the hole. They were heated in a horizontal electric furnace. With thermo-couple *C* and differential couple *D* the temperature of specimen and the temperature difference between specimen and neutral body were read on heating. Some examples of heating curves are shown in Fig. 2.

Fig. 3.

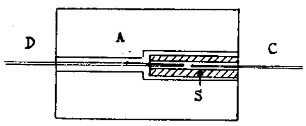

Measurement of expansion. Specimen cast in bar and annealed was heated and the expansion on heating was measured with a Konno's differential dilatometer modified as Fig. 4, i.e., the specimen and neutral body were separately placed in silica-tubes *e* and *f*, inserted in a large silica-tube *C* and they were heated in an electric furnace. Thus

Fig. 4.

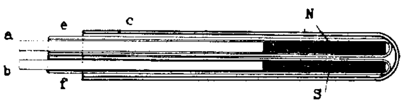

Fig. 5

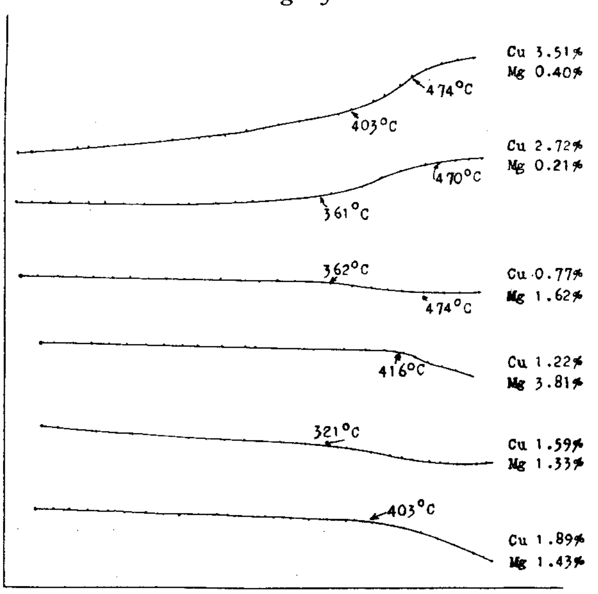

the difference of dilatation between specimen and pure Aluminium was measured and from the change point of the heating curves was determined the solubility limit of the Al solid solution. Some examples are shown in Fig. 5. We observe in these curves that some specimens expand or shrink on the dissolution of separated phase in solution.

Microscopical Examination. As usual, specimens were polished and etched with a dilute ferrous nitrate solution or a dilute hydrofluoric solution. They were examined under the microscope.

Results of thermal Analyses.

Thermal analyses were carried out on the alloys corresponding to the sections 95%, 90%, 85%, 80%, 75%, 70%, 65%, and 59% of Aluminium. The results are summarized in Table I.

The results of experiments are plotted in the sectional diagram as shown in Fig. 6–13. It is to be noticed in the thermals analysis of the ternary alloy that cooling cannot be so slow as to attain equilibrium at any instant, and consequently the reaction at the lower temperature not to occur in equilibrium are often observed. Therefore, heating thermal curves were obtained on annealed specimens according to necessity to check the solidus point. The results are also shown in Table I.

Fig. 6.
Al 94% Section

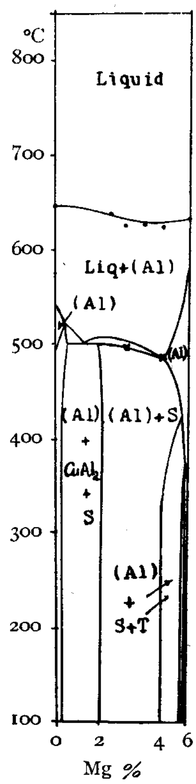

Fig. 7.
Al 90% Section

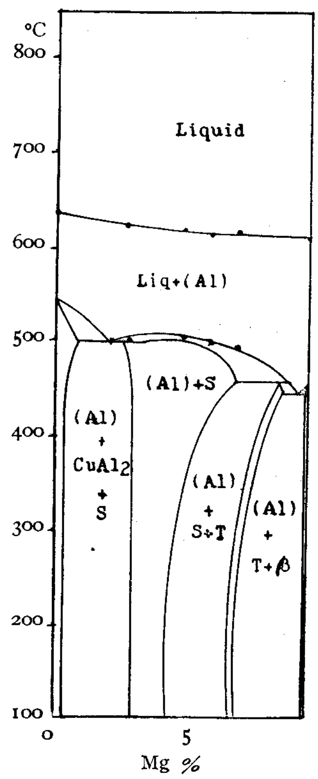

Fig. 8.

Al 85% Section

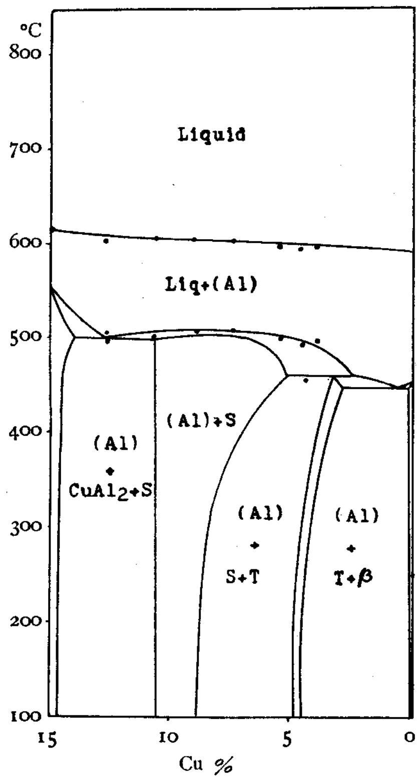

Fig. 10.

Al 75% Section

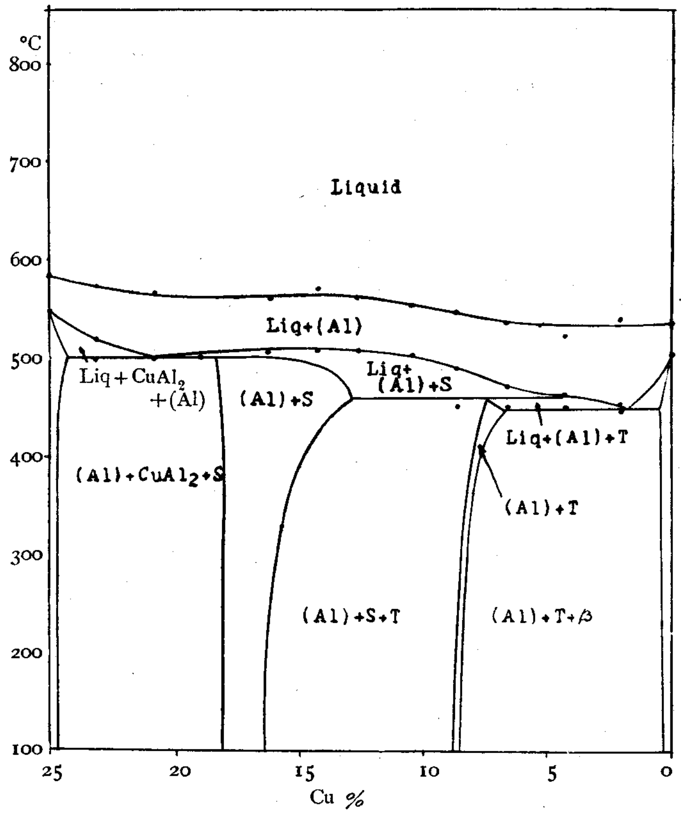

Fig. 9.

Al 80% Section

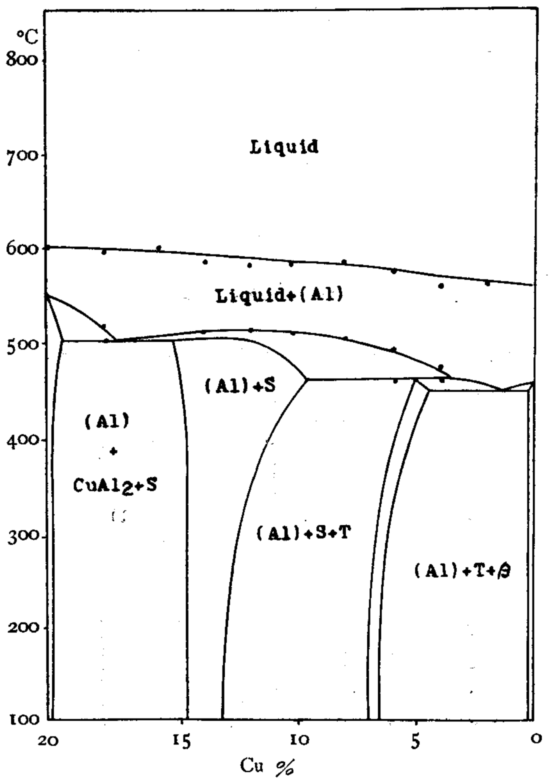

Fig. 11.

Al 70% Section

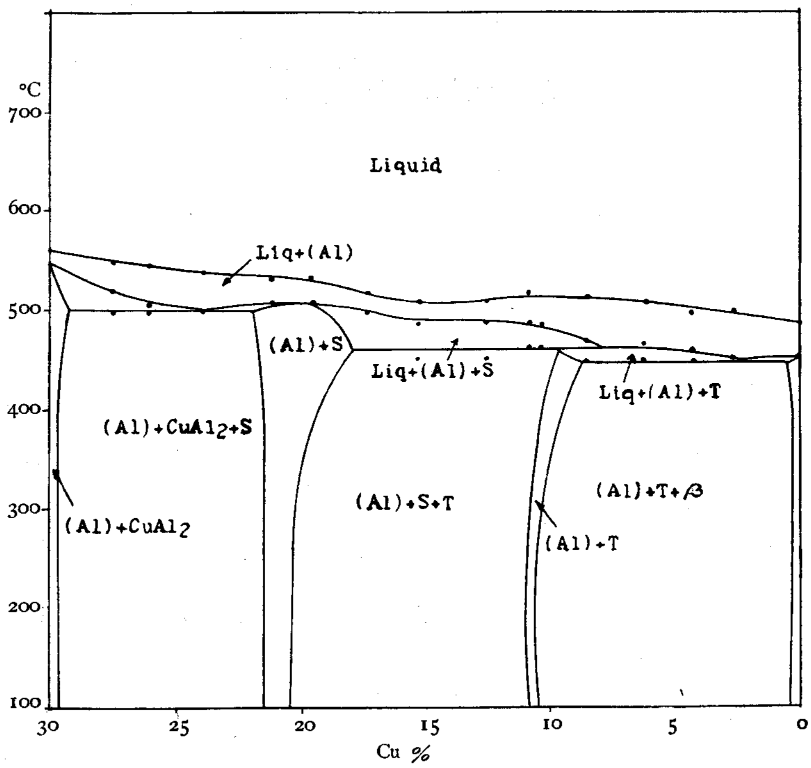

Fig. 12.
Al 65% Section

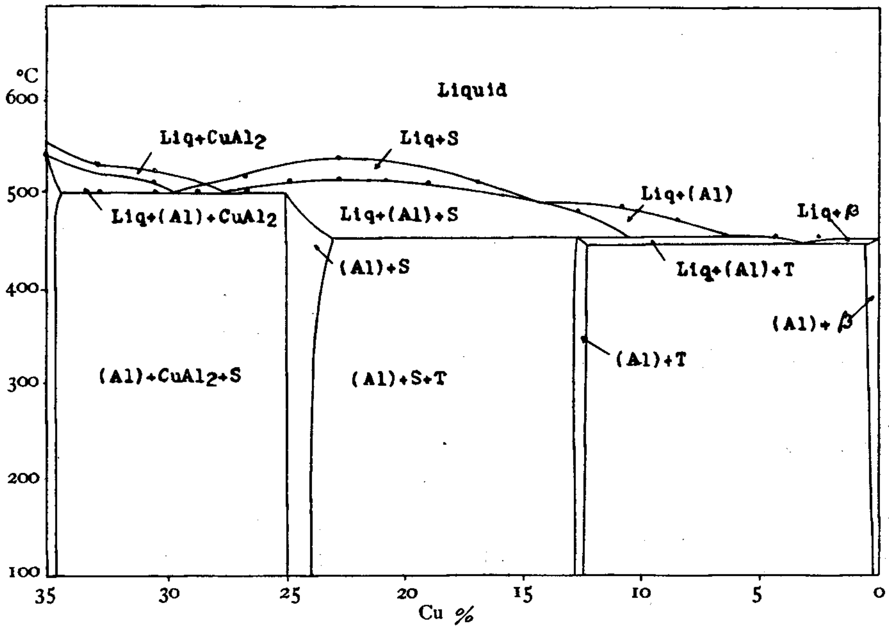

Fig. 13.
Al 49% Section

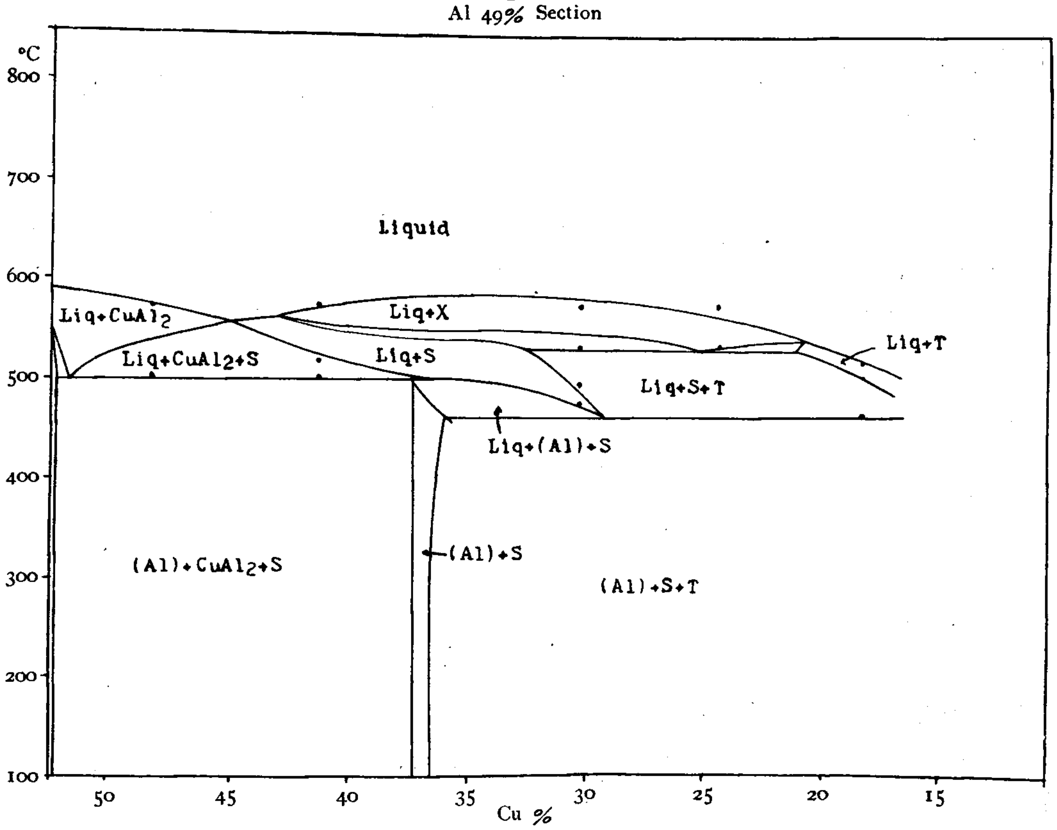

From these experiments 3 in-variant reactions are observed to occur in the sectional diagrams of Figs. 6–12. They are determined as follows:

500°C	Liquid $\rightleftharpoons$ (Al) + $CuAl_2$ + (*S*)
465°C	Liquid + (*S*) $\rightleftharpoons$ (Al) + (*T*)
447°C	Liquid $\rightleftharpoons$ (Al) + (*T*) + $(\beta)_{Al\text{-}Mg}$

where (Al) denotes the Al solid solution, and (*S*) and (*T*) are ternary compounds corresponding respectively to $Al_{13}Cu_7Mg_8$ and Al_6CuMg_4 as later explained.

In Fig. 13 an in-variant reaction at 530°C a peritecto-eutectic reaction Liquid + *X* $\rightleftharpoons$ (*S*) + (*T*), is also observed to occur, but the investigation of this section was not so complete as to determine the composition of the phase *X*. For our present purpose it was not necessary to ascertain it.

Table 1.

No.	Composition (by analysis) %			Change point °C				
	Cu	Mg	Al	on cooling				on heating
A 1	3.90	1.18	remai.	637				
A 2	3.70	2.35	"	640	493	473		
A 3	2.50	2.60	"	637				
A 4	1.75	3.50	"	628				
B 1	9.20	2.44	remai.	600	500			
B 2	7.71	2.95	"	624	498			
B 3	5.26	5.80	"	619	506			
B 4	4.02	6.07	"	615				
B 5	2.55	7.35	"	618	493			
C 1	13.00	2.04	remai.	.600	503	498		
C 2	11.10	4.12	"	605	499			
C 3	9.15	5.24	"	604	508			
C 4	7.62	7.49	"	604	506			
C 5	5.67	9.26	"	596	498			
C 6	4.66	9.68	"	591	478	454		
C 7	4.14	10.44	"	598	496			
D 1	18.50	2.48	remai.	594	515	499		
D 2	16.30	4.57	"	600	499			
D 3	14.25	6.26	"	584	508			
D 4	12.25	8.09	"	584	508			
D 5	10.25	9.66	"	581	506			
D 6	8.40	12.47	"	586	501			
D 7	6.25	14.22	"	572	492			
D 8	4.20	15.85	"	568	471	460		
D 9	2.25	18.14	"	560	547	453		
E 1	23.15	2.04	remai.	573	520	496		
E 2	20.75	4.59	"	568	494			
E 3	18.85	6.08	"	568	500			
E 4	16.60	8.53	"	562	504			
E 5	14.73	10.04	"	570	506			
E 6	12.40	12.39	"	562	505			
E 7	10.75	14.16	"	552	500			
E 8	8.55	16.00	"	542	486	459		
E 9	6.40	19.45	"	537	469	459		
E 10	4.35	20.18	"	529	462	449		
E 11	2.50	23.17	"	539	448	441		
F 1	28.05	2.20	remai.	548	522	496		
F 2	26.50	4.92	"	546	503	489		
F 3	23.82	6.16	"	537	498			
F 4	21.75	8.91	"	532	506			
F 5	19.52	10.37	"	528	506			
F 6	17.85	12.47	"	528	506			
F 7	12.55	15.46	"	518	496			
F 8	12.70	16.89	"	506	486	450		
F 9	11.05	14.52	"	520	491	464		
F 10	10.50	19.98	"	512	487	467	448	
F 11	8.80	20.31	"	513	476	468	448	
F 12	6.52	24.51	"	510	467	448		
F 13	4.05	26.15	"	495	457	448		
F 14	2.58	29.38	"	500	450			
G 1	33.15	2.12	remai.	530	498			
G 2	30.65	4.32	"	526	514	505		
G 3	28.90	6.38	"	528	506			
G 4	27.25	8.47	"	520	512	506		
G 5	25.00	10.47	"	515				
G 6	23.15	12.51	"	542	515			
G 7	20.70	13.98	"	512	464			
G 8	18.75	16.08	"	510	466			
G 9	16.82	18.10	"	514	466			
G 10	14.55	20.72	"	490	468	446		
G 11	12.50	22.06	"	482	466	448		
G 12	11.75	23.87	"	484	466	448		
G 13	8.30	26.48	"	472	448			
G 14	6.20	28.87	"	458	446			
G 15	4.35	31.07	"	454				
G 16	2.15	32.29	"	452	448			
H 1	48.59	3.36	remai.	570	540	500		
H 2	41.74	10.78	"	575	543	515	502	
H 3	27.92	20.75	"	573	530	493	475	
H 4	23.42	25.25	"	575	530			
H 5	18.30	31.00	"	520	502	463		
I 1	27.28	14.63	remai.					478
I 2	23.85	16.62	"					477
I 3	21.09	18.81	"					463
I 4	16.56	25.45	"					460
I 5	13.07	28.88	"					455
I 6	11.16	30.17	"					455
I 7	8.20	33.90	"					455
I 8	6.19	35.04	"					454
I 9	2.96	37.14	"					454

Table 2.

No.	Composition (by analysis) %			Change point °C				
	Cu	Mg	Al	on cooling				on heating
P 1	3.51	0.40	remai.	625				
P 2	4.74	0.94	"	617				
P 3	5.62	1.07	"	612	497			
P 4	6.73	1.27	"	600	497			
P 5	13.00	2.04	"	600	503	498		
P 6	18.50	2.48	"	594	515	499		
P 7	30.65	4.32	"	526	514	505		
Q 1	1.51	0.12	remai.					562
Q 2	2.56	0.65	"	638				550
Q 3	6.01	1.72	"	620	490			500
Q 4	9.20	2.44	"	620	500			500
Q 5	20.75	4.59	"	568	494			
Q 6	23.82	6.16	"	537	498			
Q 7	28.90	6.38	"	528	506			
R 1	1.63	0.94	remai.	651				
R 2	1.94	1.17	"	648				505
R 3	2.81	1.74	"	646				503
R 4	4.01	2.40	"	644	498			503
R 5	4.90	2.90	"	642	497			501
R 6	14.25	6.26	"	584	508			
R 7	16.60	8.53	"	562	504			
S 1	1.12	0 82	remai.	646				610
S 2	1.59	1.33	"	644				596
S 3	1.89	1.42	"	642				
S 4	2.37	1.87	"	640				500
S 5	3.13	2.34	"	638	495			500
S 6	4.40	3.22	"	635	500			503
S 7	9.15	5.24	"	604	508			
S 8	12.25	8.09	"	584	508			
S 9	14.73	10.04	"	570	506			
S 10	17.85	12.47	"	528	506			
S 11	23.15	12.51	"	542	515			
T 1	0.43	0.21	remai.	646				
T 2	1.33	1.75	"	645				550
T 3	2.02	1.93	"	630				540
T 4	2.50	2.60	"	637				500
T 5	3 08	3.13	"	620	495			498
T 6	4.08	4 08	"	615	488			498
T 7	5.26	5.80	"	619	506			
T 8	7.62	7.49	"	604	506			
T 9	10.25	9.66	"	581	506			
T 10	12.40	12.39	"	526	505			
T 11	15.25	15 46	"	518	496			
U 1	0.81	1.11	remai.	651				566
U 2	1.23	1.64	"	647				533
U 3	1.42	1.98	"	644				
U 4	1.57	2.35	"	640				527
U 5	1.72	2.75	"	637	490			508
U 6	2.74	3.83	"	630	573	492		506
U 7	4.02	6.07	"	615				506
U 8	5.67	9.26	"	596	498			
U 9	8.55	16.00	"	546	486	459		
U 10	11.05	19.52	"	520	500	491	464	
U 11	12.50	22.06	"	482	466	448		
V 1	0.77	1.62	remai.	645				588
V 2	1.22	3.81	"	632				515
V 3	1.74	4.61	"	625				487
V 4	2.73	6.87	"	610				500
V 5	3.20	8.08	"	613				487
V 6	4.14	10.44	"	598	496			
V 7	6.23	14.20	"	.572	492	458		
V 8	8.80	20.31	"	513	476	468	448	
W 1	0.80	5.46	remai.	635				508
W 2	0.83	7.13	"	627				491
W 3	1.12	8.50	"	612				488
W 4	1.32	10.24	"	608	473			
W 5	1.68	11.20	"	603	470			
W 6	2.10	12.92	"	624	490			
W 7	2.25	18.14	"	610	577	493		
W 8	4.05	26.15	"	495	457	448		
W 9	4.35	31.07	"	454				

Remarks : remai. = remainder.

Fig. 14.

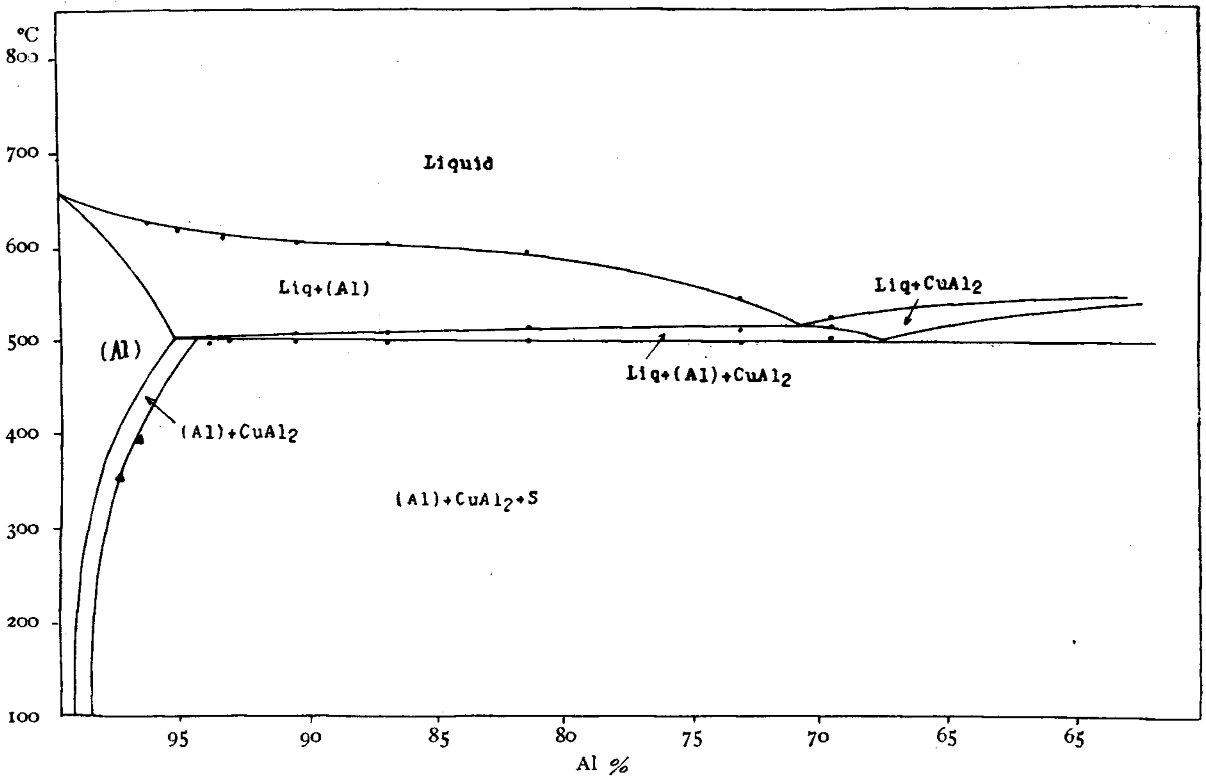
°C
800
700
600
500
400
300
200
100
Liquid
Liq+(Al)
Liq+CuAl2
(Al)
Liq+(Al)+CuAl2
(Al)+CuAl2
(Al)+CuAl2+S
95
90
85
80
75
70
65
65
Al %

Fig. 15.

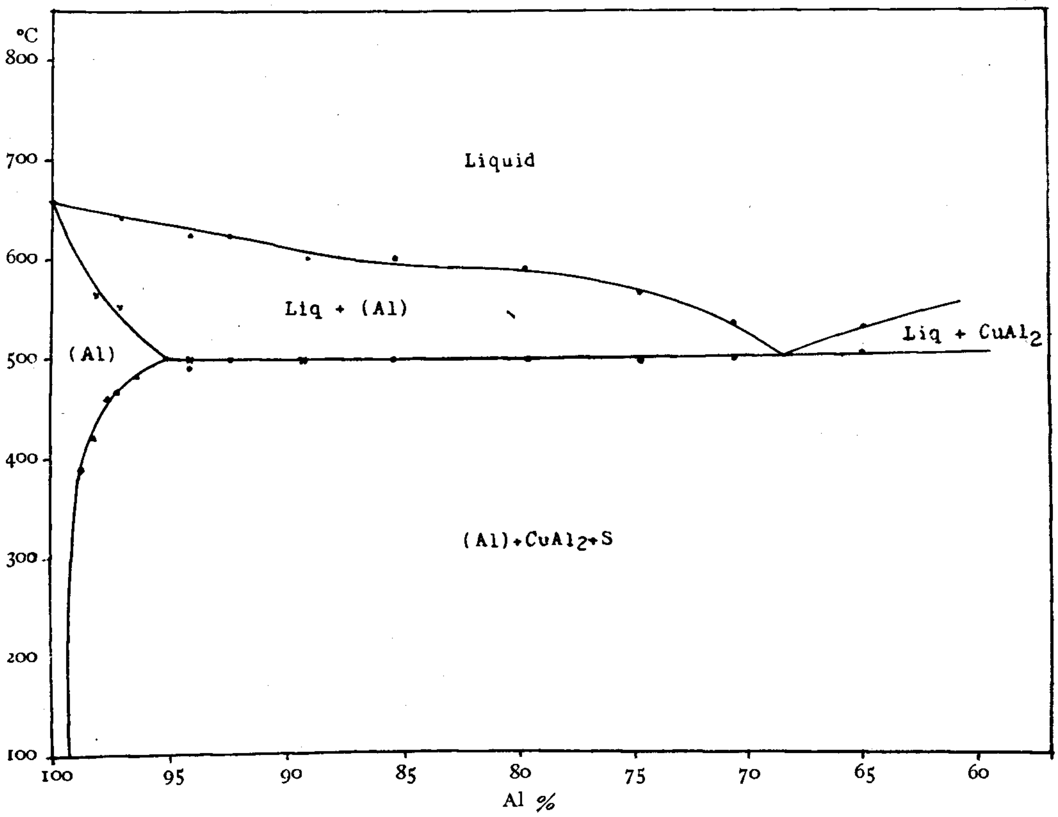
°C
800
700
600
500
400
300
200
100
Liquid
Liq + (Al)
(Al)
Liq + CuAl2
(Al)+CuAl2+S
100
95
90
85
80
75
70
65
60
Al %

Fig. 16.

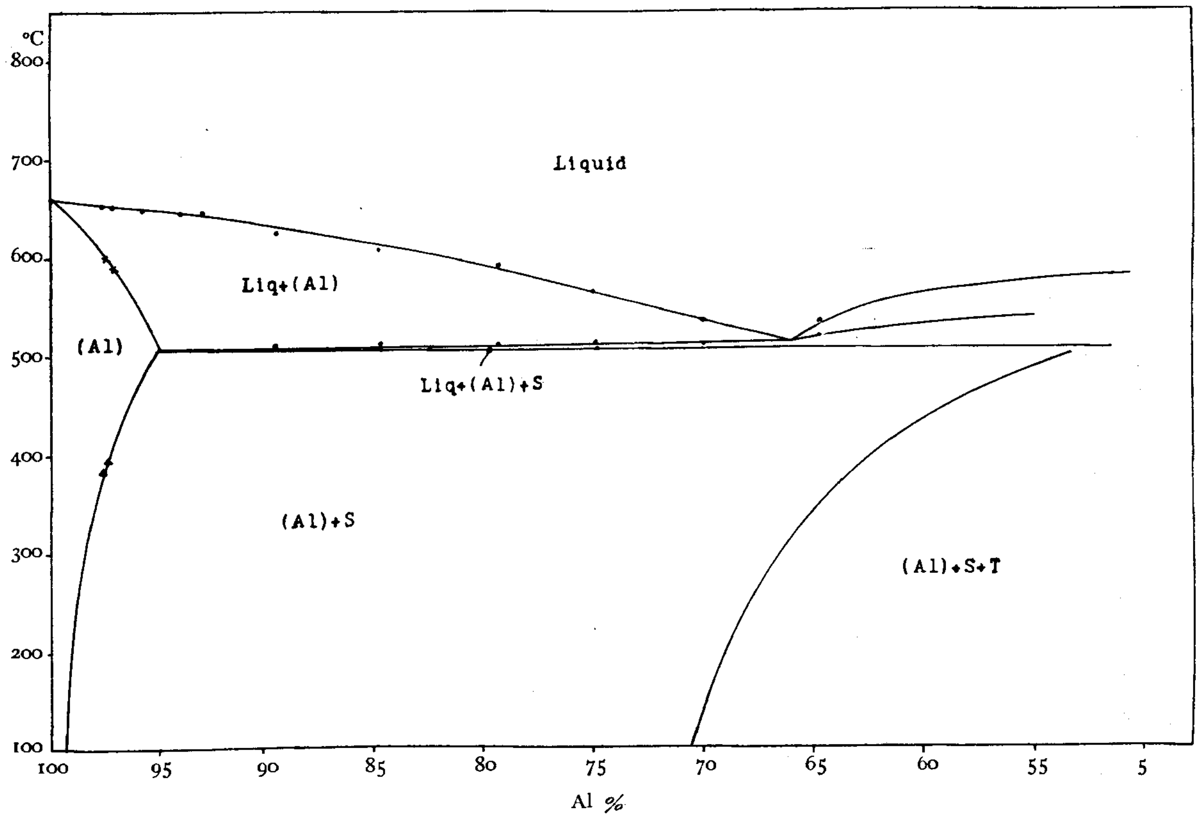
°C
800
700
600
500
400
300
200
100
Liquid
Liq+(Al)
(Al)
Liq+(Al)+S
(Al)+S
(Al)+S+T
100
95
90
85
80
75
70
65
60
55
5
Al %

Fig. 17.

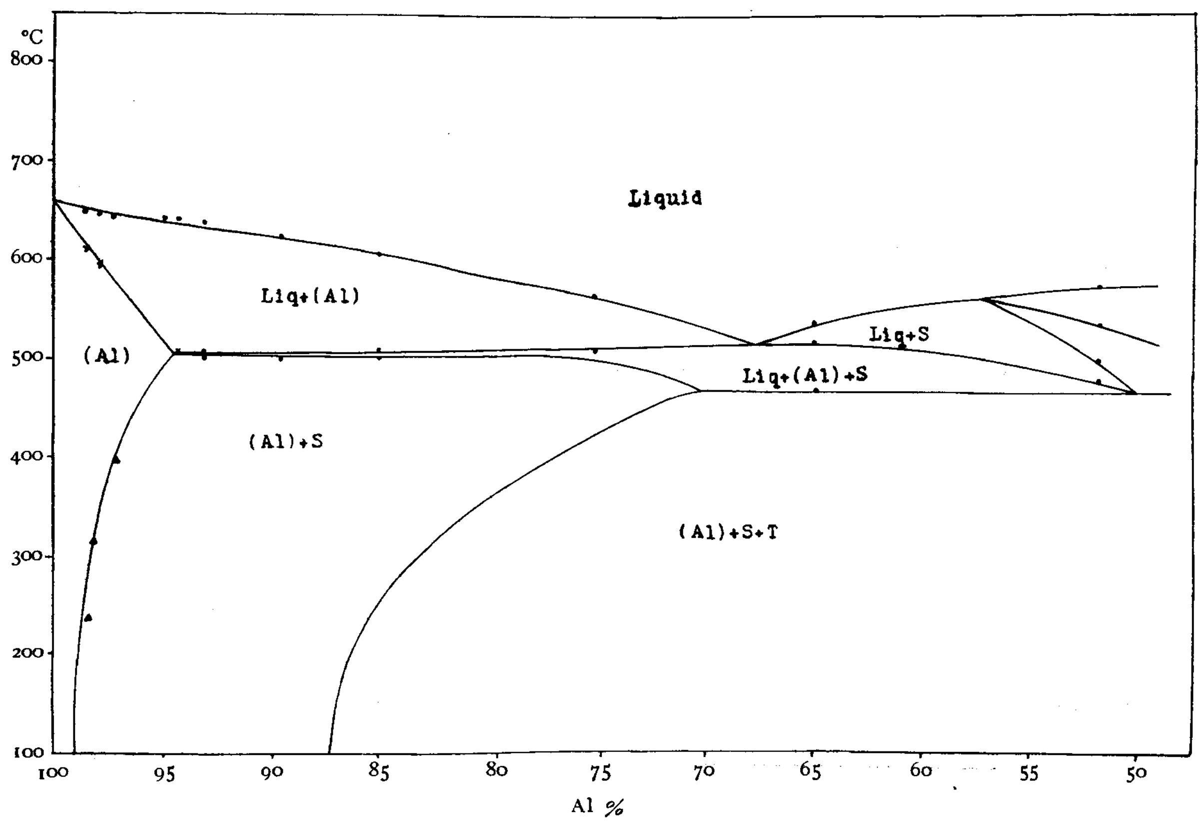
°C
800
700
600
500
400
300
200
100
Liquid
Liq+(Al)
(Al)
Liq+S
Liq+(Al)+S
(Al)+S
(Al)+S+T
100
95
90
85
80
75
70
65
60
55
50
Al %

Fig. 18.

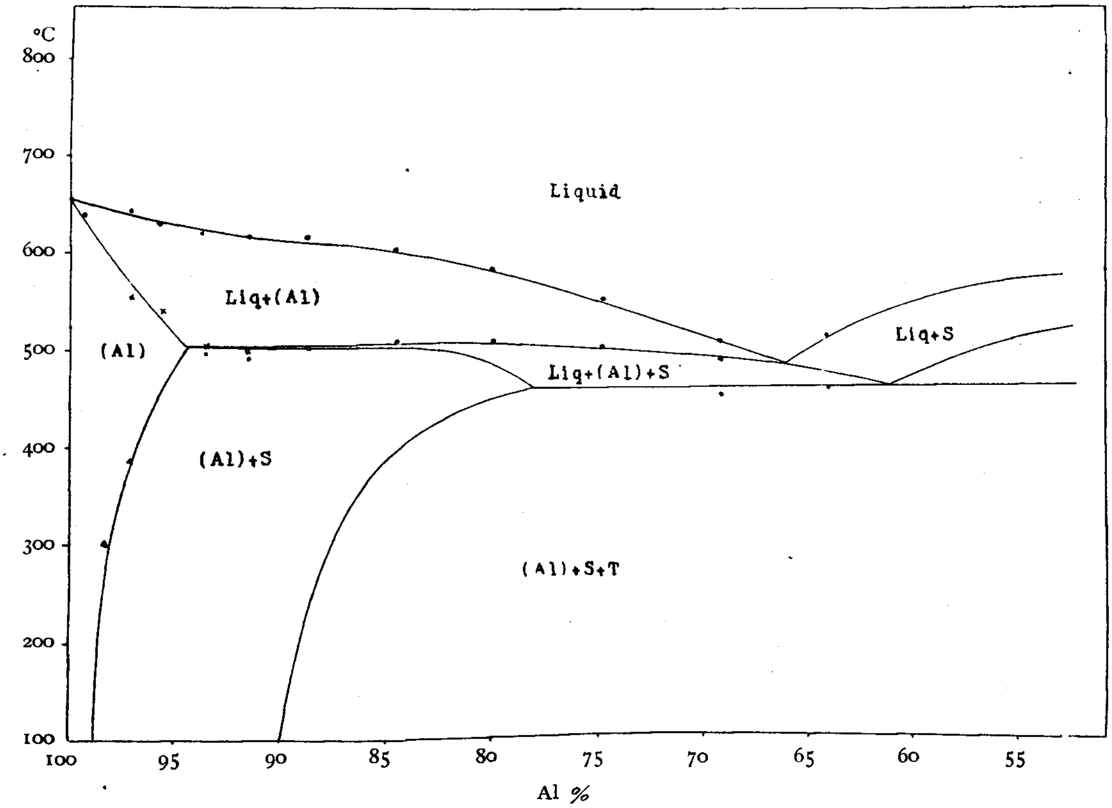
°C
800
700
600
500
400
300
200
100
Liquid
Liq+(Al)
(Al)
Liq+S
Liq+(Al)+S
(Al)+S
(Al)+S+T
100
95
90
85
80
75
70
65
60
55
Al %

Fig. 19.

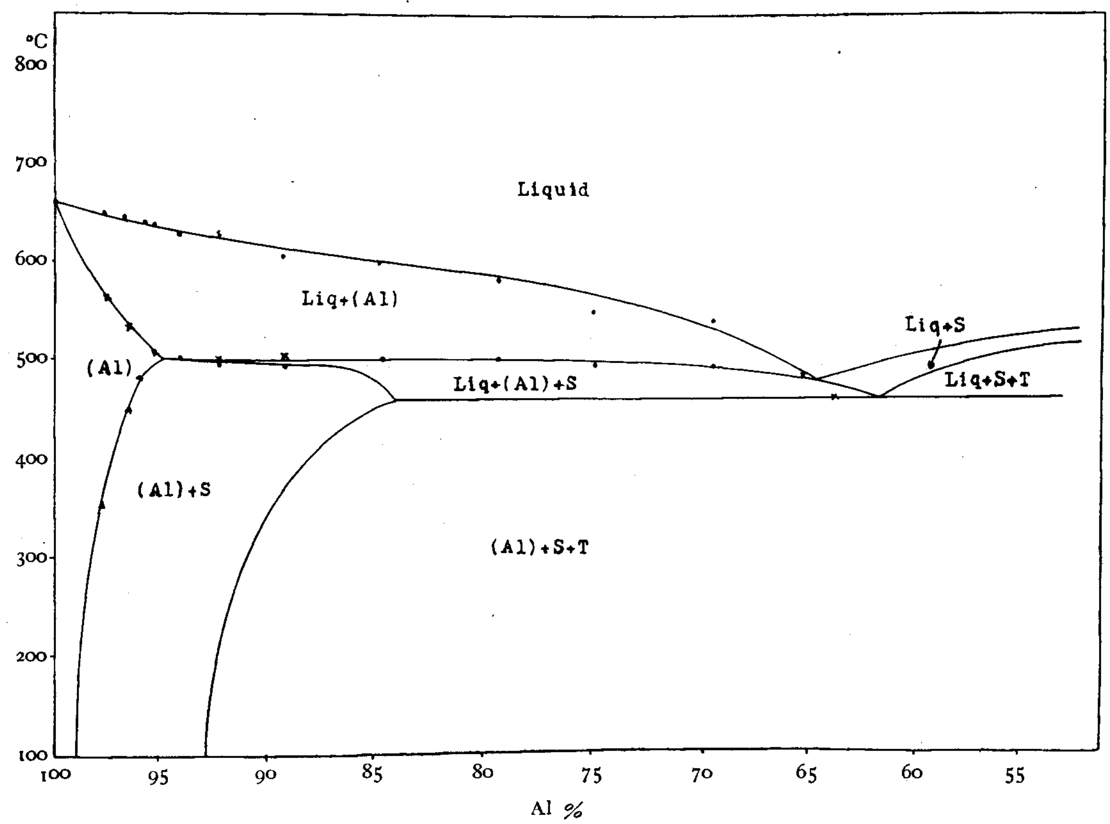
°C
800
700
600
500
400
300
200
100
Liquid
Liq+(Al)
Liq+S
(Al)
Liq+(Al)+S
Liq+S+T
(Al)+S
(Al)+S+T
100
95
90
85
80
75
70
65
60
55
Al %

Fig. 20.

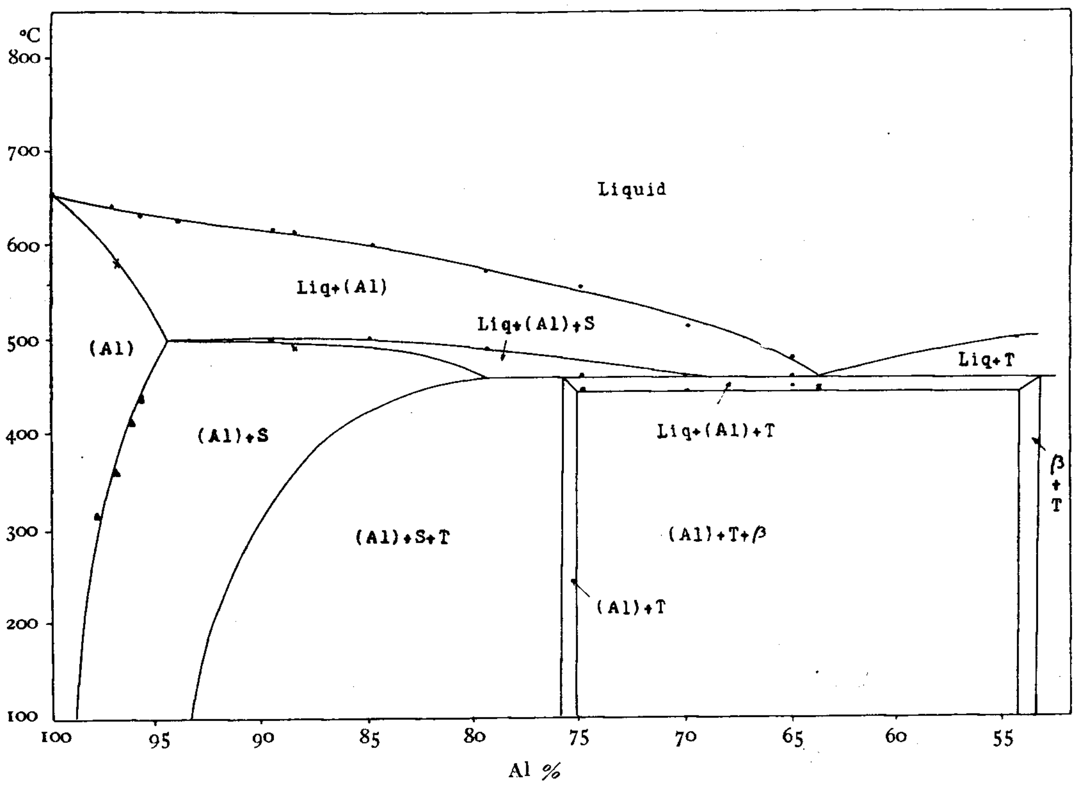
°C
800
700
600
500
400
300
200
100
Liquid
Liq+(Al)
Liq+(Al)+S
Liq+T
(Al)
(Al)+S
Liq+(Al)+T
β
+
T
(Al)+S+T
(Al)+T+β
(Al)+T
100
95
90
85
80
75
75
70
65
60
55
Al %

Fig. 21.

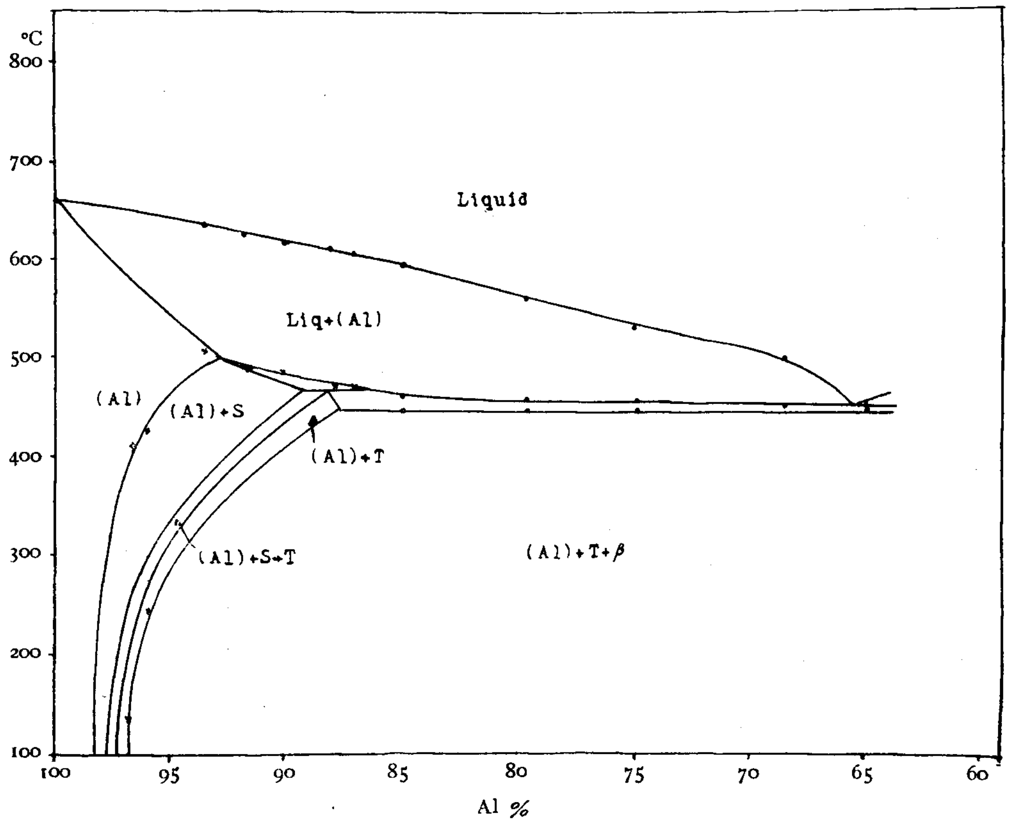
°C
800
700
600
500
400
300
200
100
Liquid
Liq+(Al)
(Al)
(Al)+S
(Al)+T
(Al)+S+T
(Al)+T+β
100
95
90
85
80
75
70
65
60
Al %

The results of thermal analyses on the alloys corresponding to the 8 sections passing Al-axis are summarized in Table 2 and they are plotted in Figs. 14–21.

Measurement of thermal expansion.

Chill cast bars were annealed at 500°C at least during 16 hours and then at 150°C during 1 week. They were heated with Al bar as neutral body. The difference of dilation was measured. As shown in Fig. 4, we observed sharp change of direction on these heating curves, and from these change points the solid solubility limit was determined The results of experiments are given in Table 3. The results are plotted in Fig. 14–21.

Table 3.

No.	Composition (by axalysis) %			Change point °C	
	Cu	Mg	Al		
PS 1	2.72	0.21	remainder	361	460
PS 2	3.51	0.40	"	403	472
QS 1	1.10	0.26	remainder	390	
QS 2	1.50	0.12	"	420	
QS 3	2.20	0.49	"	460	
QS 4	2.56	0.65	"	466	
QS 5	3.72	1.05	"	480	
RS 1	1.63	0.94	remainder	396	
RS 2	1.94	1.17	"	403	
SS 1	1.12	0.82	remainder	238	
SS 2	1.59	1.33	"	305	
SS 3	1.89	1.43	"	397	
TS 1	0.98	1.11	remainder	305	
TS 2	1.13	1.75	"	387	
US 1	0.81	1.11	remainder	360	
US 2	1.23	1.64	"	455	
US 3	1.42	1.98	"	486	
VS 1	0.49	1.16	remainder	315	
VS 2	0.77	1.62	"	360	
VS 3	1.06	2.34	"	411	
VS 4	1.22	3.81	"	436	
WS 1	0.40			132	416
WS 2	0.42			248	425

It is noted from these results that the maximum solubility of Cu and Mg decreases in the ternary alloys, compared with that of binary alloys. The solid solubility of Al solution decreases from the higher temperature to the lower, but the degree of decrease differs in each sectional diagram. In section Fig. 15 the solubility decreases in a marked degree from the higher temperatures to the lower, but in the section Fig. 6 the decrease is not so sharp.

Specimens containing Cu 3.51% and Mg 0.40% show contraction with the dissolution of separated phases in solution as shown in Fig. 4. The separated phases in these specimens are $CuAl_2$ and *S*-compound. It is considered that the *S*-compound is not so much separated as $CuAl_2$, in considering the content of Mg. The contraction above observed may be due to the dissolution of $CuAl_2$ in Al.

However, the specimens containing Cu 1.22% and Mg 3.81% expand with the dissolution of separated phases in solution. The separated phase is evidently *S*-compound as seen in Fig. 20: hence this expansion must be due to the dissolution of *S*-compound in Al.

Microscopical examination.

From the thermal analyses and the measurement of thermal expansion, the equilibrium diagram of this system has been almost determined. Therefore, microscopical examination was exployed to ascertain these results. Some important results are shown in Fig. 22.

In Vogel's diagram, there exists a ternary compound Al_6CuMg_4 as the phase to be in equilibrium with Al. But in our experiments 2 ternary compounds were found to exist, from the examination of many annealed specimens. Fig. 22 (a) and (b) shows the micro-photographs of these alloys. Their compositions were found to be Mg 17.07% and Cu 44.37%, and Mg 33.05% and Cu 19.43% respectively, by chemical analysis. Therefore they were determined to be $Al_{13}Cu_7Mg_8$ and Al_5CuMg_4. The present writer denotes them *S* and *T* respectively.

Fig. 22 (c) shows a micro-structure of an alloy containing Cu 18.50% and Mg 2.48% which was annealed at 450°C for 48 hours. This alloy crystallizes with ternary eutectic reaction

$$\text{Liquid} \rightarrow (Al) + CuAl_2 + S$$

after the primary separation of (Al) and the binary eutectic reaction Liquid→(Al)+ $CuAl_2$. Therefore this alloy consists (Al), $CuAl_2$ and *S*-compound. It is distinctly seen in the photograph, i.e., the Al solid solution as the matrix, the $CuAl_2$ in half-tone and the black crystals of *S*-compound. Actually the $CuAl_2$ and the *S*-compound are coloured reddish brown by dilute ferrous nitrate solution, but *S*-compound is etched in deep red-brown, while the colour of $CuAl_2$ is pale red-brown. Thus they are distinguished from each other in the microstructure.

The alloy D3 containing Cu 14.25% and Mg 6.26% solidifies into a mixture of (Al)+*S* after the primary separation of (Al). Fig. 22 (d) shows such a structure consisting of (Al)-solid solution and *S*-compound, the latter being etched in deep red-brown colour.

Fig. 22 (e) shows the microstructure of the alloy D6 (Cu 8.40%, Mg 12.47%) consisting of primary (Al)-crystals, binary eutectic mixtures (Al)+*S*, and ternary complex solidified by the

Fig. 22.

(a)

Cu 44.37%, Mg 17.07%, Al balance. ×150. Etched with ferrous nitrate sol.

(b)

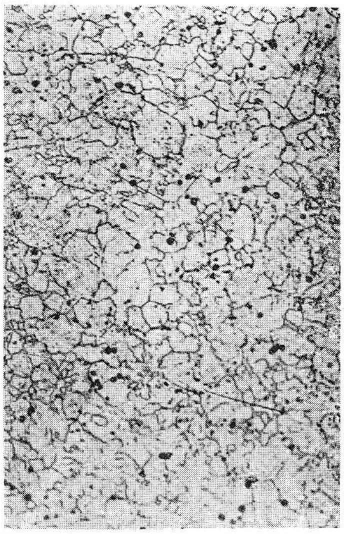

Cu 19.43%, Mg 33.05%, Al balance. ×150. Etched with HF sol.

(c)

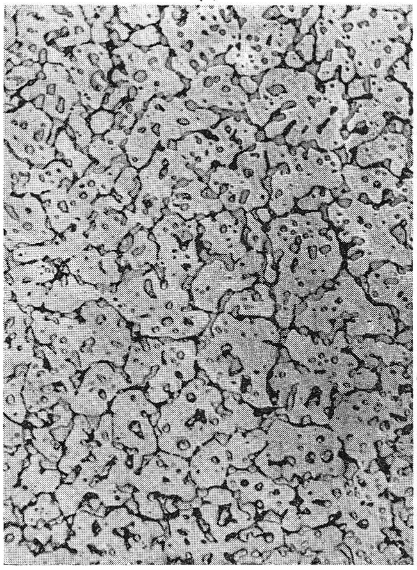

P6. Cu 18.50%, Mg 24.80%, Al balance. ×150. Annealed for 48 hrs. at 450°C. Etched with ferrous nitrate sol.

(d)

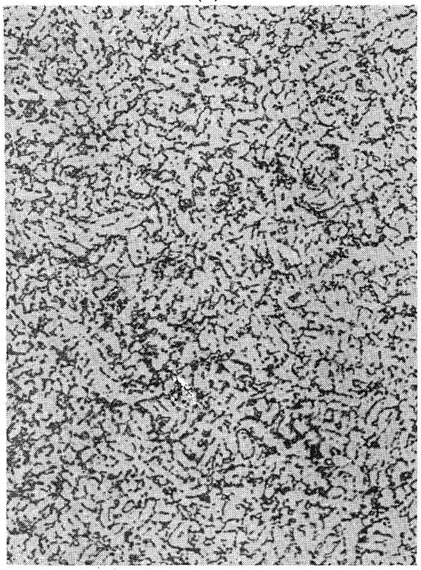

D3. Cu 14.25%, Mg 6.26%, Al balance. ×150. Annealed for 48 hrs. at 450°C. Etched with ferrous nitrate sol.

(e)

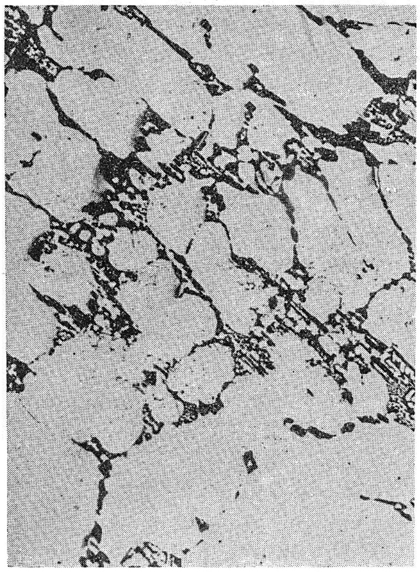

D6. Cu 8.40%, Mg 12.47%, Al balance. ×150. Annealed for 48 hrs. at 450°C. Etched with ferrous nitrate sol.

(f)

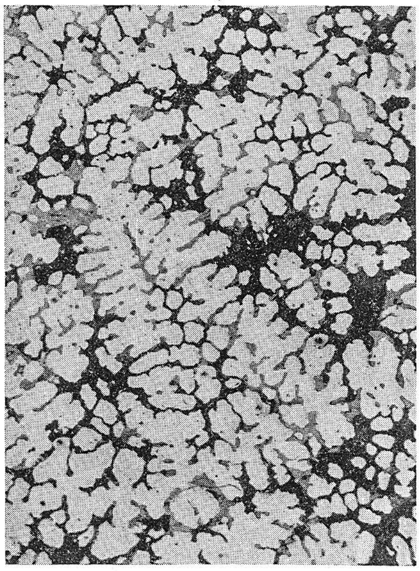

D9. Cu 2.25%, Mg 18.14%, Al balance. ×150. Etched with ferrous nitrate sol.

(g)

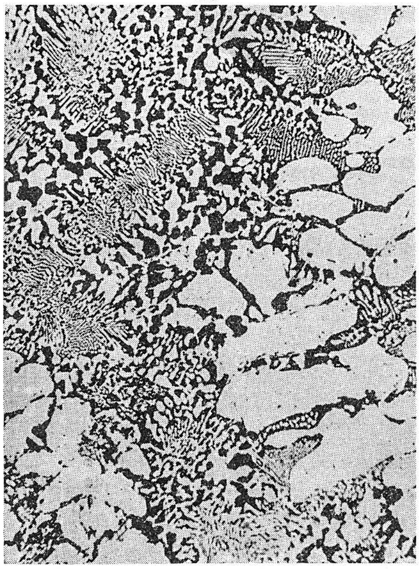

E4. Cu 16.60%, Mg 8.53%, Al balance. Cooled in furnace. ×150. Etched with ferrous nitrate sol.

(h)

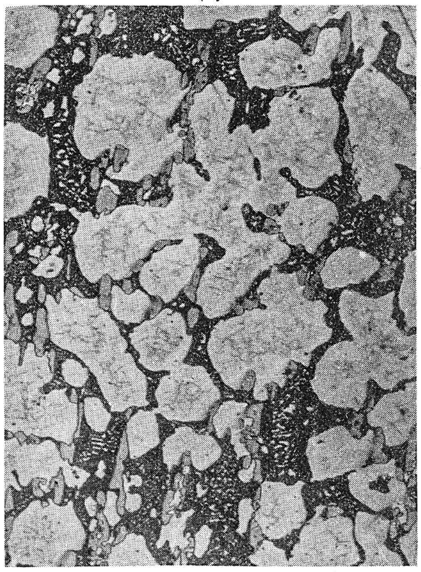

E8. Cu 8.55%, Mg 16.00%. Al balance. Cooled in Furnace. ×150. Etched with HF sol.

(i)

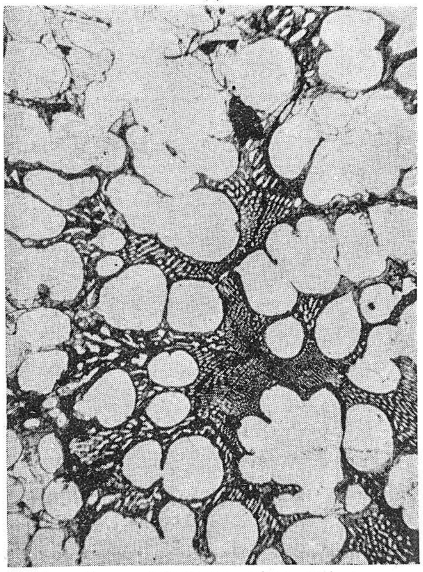

E10. Cu 4.35%, Mg 20.18%, Al balance. Cooled in Furnace. ×150. Etched with HF sol.

(j)

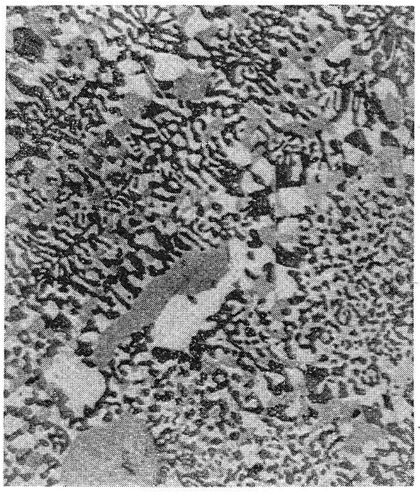

G2. Cu 30.65%, Mg 4.32%, Al balance. Cooled in furnace. ×300. Etched with ferrous nitrate sol.

(k)

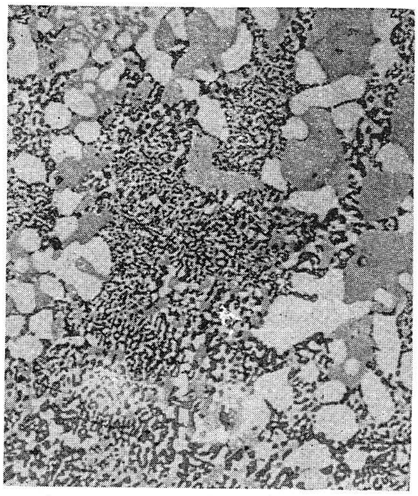

G2. Cu 30.65%, Mg 4.32%, Al balance. Cooled in furnace. ×150. Etched with ferrous nitrate sol.

(l)

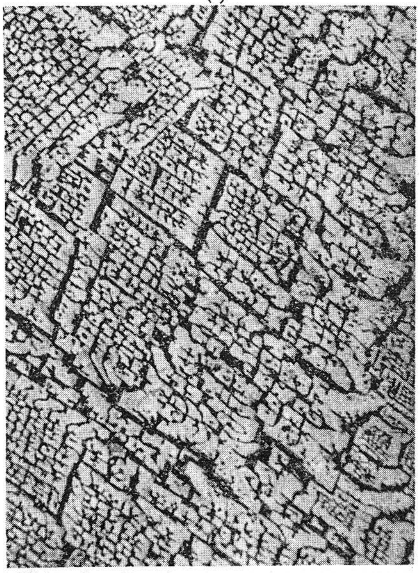

H1. Cu 48.59%, Mg 3.36%, Al balance. Cooled in furnace. ×150. Etched with HF sol.

(m)

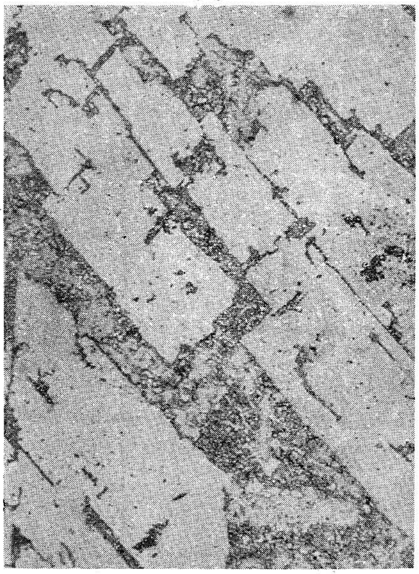

H1. Cu 48.59%, Mg 3.36%, Al balance. Chill cast. ×150. Etched with HF. sol.

(n)

Cu 35.0%, Mg 5.0%, Al balance. Cooled in furnace. ×150. Etched with ferrous nitrate sol.

(o)

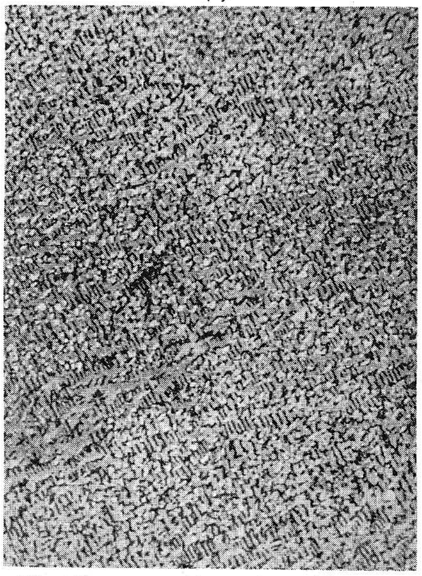

H2. Cu 41.74%, Mg 10.78%, Al balance. Chill cast. ×150. Etched with ferrous nitrate sol.

(p)

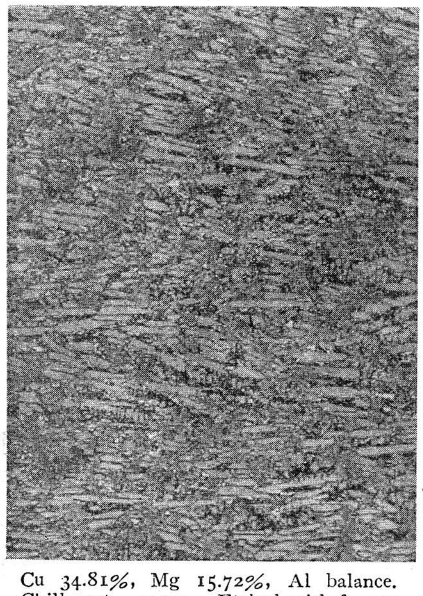

Cu 34.81%, Mg 15.72%, Al balance. Chill cast. ×150. Etched with ferrous nitrate sol.

(q)

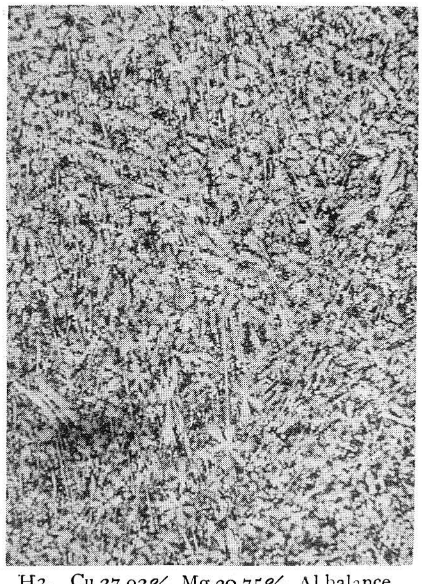

H3. Cu 27.92%, Mg 20.75%, Al balance. Chill cast. ×150. Etched with HF. sol.

(r)

Cu 19.45%, Mg 23.67%, Al balance. Chill cast. ×150. Etched with HF. sol.

(s)

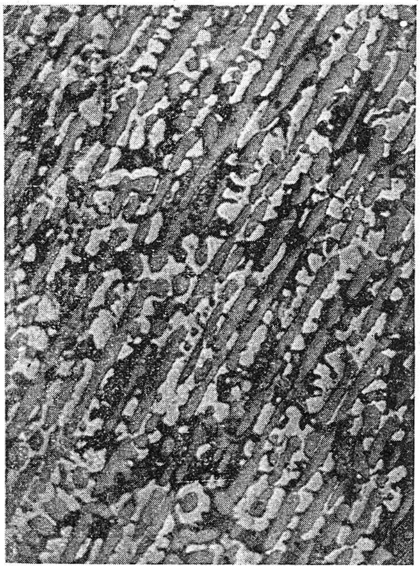

I2. Cu 23 85%, Mg 16.62%, Al balance. Cooled in furnace. ×150. Etched with ferrous nitrate sol.

(t)

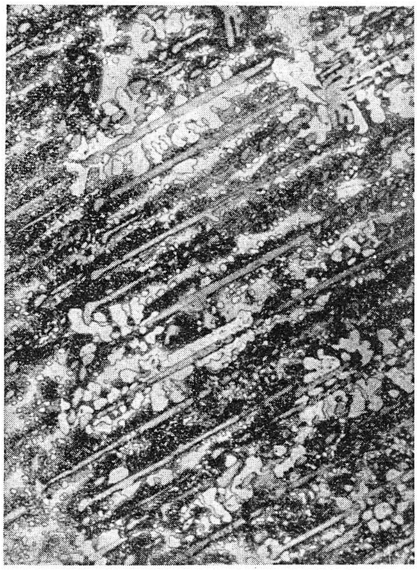

I4. Cu 16.56%, Mg 25.45%, Al balance. Cooled in furnace. ×150. Etched with ferrous nitrate sol.

(u)

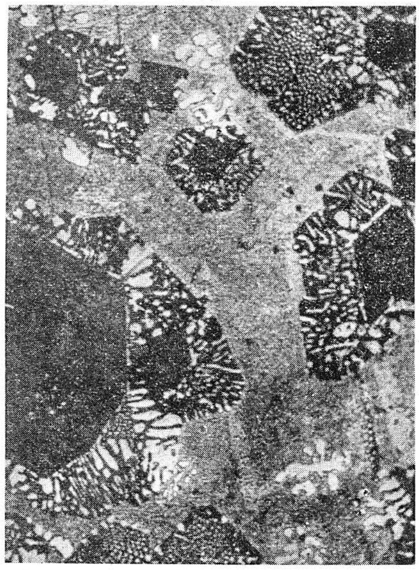

Cu 11.16%, Mg 30.17%, Al balance. Cooled in furnace. ×150. Etched with HF sol.

Fig. 23.

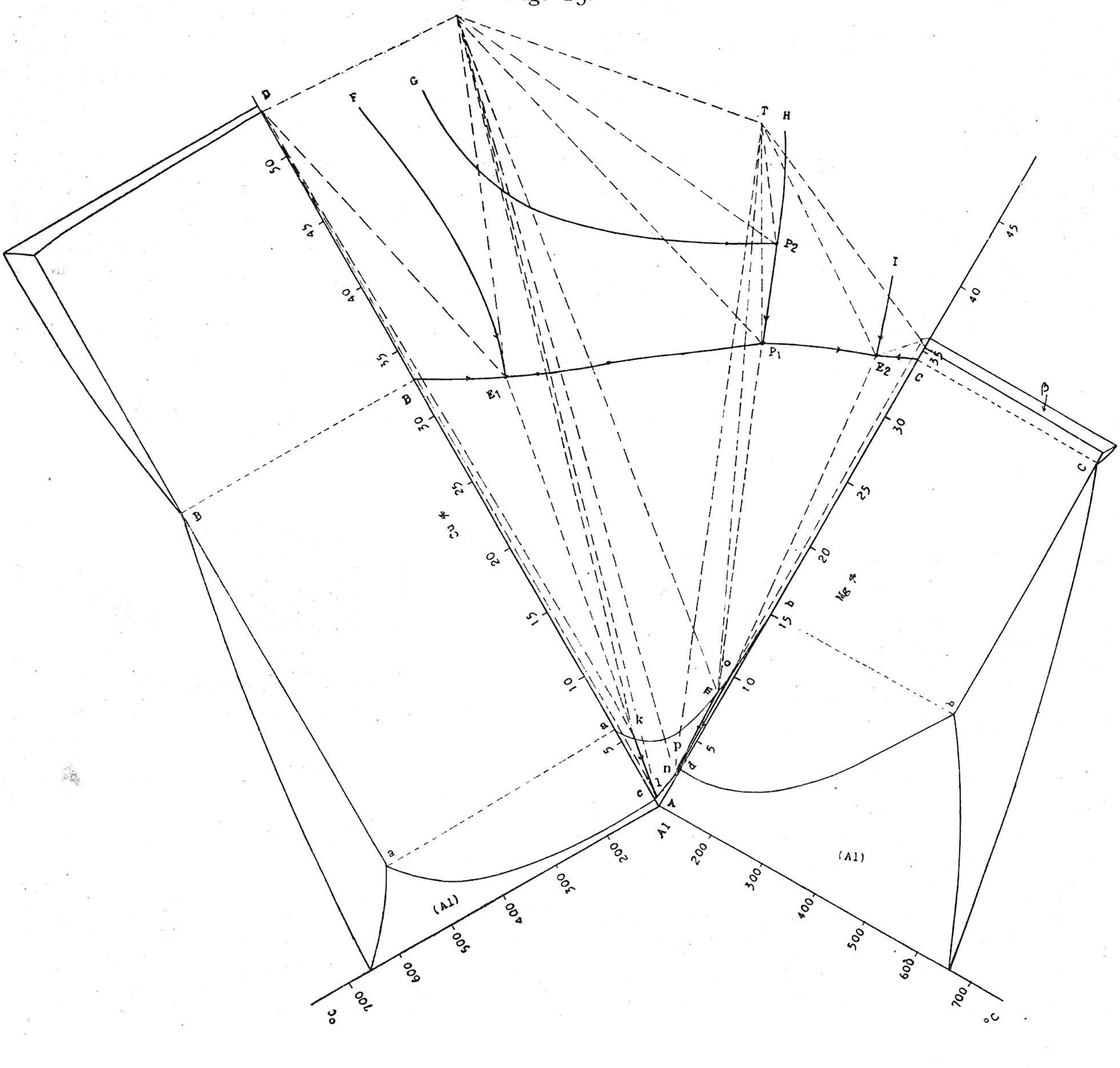

reaction Liquid + $S \rightarrow$ (Al) + T. Fig. 22 (f) is a micro-photograph which shows the primarily separated (Al), the binary eutectic mixture (Al) + T and the ternary eutectic (Al) + T + $(\beta)_{Al\text{-}Mg}$. The (Al) is the white dendritic crystals, which are surrounded by the compound T in half-tone colour and the black ground of ternary mixtures.

The alloy E4 (Cu 16.60%, Mg 8.53%) crystallizes by the eutectic reaction liquid $\rightarrow$ (Al) + S after the primary separation of (Al). Its microstructure therefore, consists of Al-dendrites surrounded by the mixture (Al) + S as shown in Fig. 22 (g). In the alloy E8 (Cu 8.55%, Mg 16.0%), (Al) separates primarily, next the binary eutectic Liquid $\rightarrow$ (Al) + S occurs and it solidifies by the reaction Liquid + $S \rightarrow$ (Al) + T. This is shown in Fig. 22 (h), in which (Al) primary crystals are surrounded by S-compounds and the black portions in the matrix are T-compound. In this matrix, small crystals of (Al) and S are also observed. E10 (Cu 4.35%, Mg 20.18%) crystallizes similarly as the alloy D9. Its microstructure is shown in Fig. 22 (i).

The Figs. 22 (j) and (k) are shown especially to distinguish $CuAl_2$ from S-compound in the ternary eutectic (Al) + $CuAl_2$ + S. They are the microstructures of the alloy G2 (Cu 30.65%, Mg 4.32%) under the magnification of 150 and 300 diameters. In this structure, the Al-primary crystals are separated in a small quantity, while the binary eutectic (Al) + $CuAl_2$ and the ternary eutectic (Al) + $CuAl_2$ + S develop considerably. It is distinctly seen that this ternary eutectic consists of white (Al) crystals, $CuAl_2$ in half-tone colour, and black S-compounds. From these photographs the existence of S-compound is also evident.

The alloy containing Cu 48.59% and Mg 3.36% separates primarily the $CuAl_2$. This is shown in Fig. 22 (l). The angular crystals are $CuAl_2$. Fig. 22 (m) is the microstructure of the same alloy cooled in a furnace, in which the primary $CuAl_2$ are surrounded by binary and ternary eutectic mixtures.

The alloy containing Cu 35% and Mg 5% crystallizes similarly as the above alloy, but in this alloy the binary and the ternary eutectic are developed in marked degree as shown in Fig. 22 (n).

Fig. 22 (o) shows the microsctructure of the chill-cast alloy containing Cu 41.74% and Mg 10.78%, in which S-compound separates primarily as shown in Fig. while in the alloy containing Cu 34.81%, and Mg 15.72%, separates an unknown phase X, and S-compounds are produced by the reaction Liquid + $X \rightarrow S$, as shown in Fig. 22 (p). In the figure the unknown crystals X are observed to exists in star-like forms and the S-compounds in long needle crystals. Both of them are etched in red-brown by ferrous nitrate solution: hence they are hardly distinguished by the etched colours. The unknown crystals are distantly observed in Fig. 22 (q) because they are much developed in the alloy containing Cu 27.92% and Mg 20.75%.

Fig. 22 (r) is an example of the microstructure of such an alloy which separates S-compounds primarily and after the eutectic reaction Liquid $\rightarrow$ S + (Al) it solidifies with the peritecto-eutectic reaction liquid + $S \rightarrow$ (Al) + T. The primarily-separated S-compound in needle forms are surrounded by dendritic Al-crystals, and the matrix in composed of the ternary mixtures produced by peritecto-eutectic reaction.

The alloy containing Cu 23.85% and Mg 16.62% crystallizes in a similar manner, but it separates more of S-compounds as the primary crystals. It is illustrated in Fig. 22 (s) and Fig. 22 (t) is a similar one.

Fig. 22 (u) represents a microstructure of an alloy containing Cu 11.16% and Mg 30.17%. The black angular crystals are the primarily-separated T-compounds surrounded by the binary eutectic mixture (Al) + T, in the matrix of (Al) + T + β.

Summing up the present experimental results, we obtained a general equilibrium diagram as shown in Fig. 23. In the figure, $BACE_2P_1E_1$ represents a field of the primary separation of aluminium and those of $CuAl_2$, S, T, β and X are respectively shown by DBE_1F, $FE_1P_1P_2G$, $HP_2P_1E_2I$, IE_2C and GP_2H.

The binary complex lines showing the univariant reactions in the figure are summarized as follows.

BE_1	$Liquid_{BE_1} \rightleftharpoons (Al)_{ak} + CuAl_2$
E_1P_1	$Liquid_{E_1P_1} \rightleftharpoons (Al)_{km} + S$
P_1E_2	$Liquid_{P_1E_2} \rightleftharpoons (Al)_{mo} + T$
CE_2	$Liquid_{CE_2} \rightleftharpoons (Al)_{bo} + \beta$
FE_1	$Liquid_{FE_1} \rightleftharpoons CuAl_2 + S$
P_2P_1	$Liquid_{P_2P_1} \rightleftharpoons T + S$
GP_2	$Liquld_{GP_2} + X \rightleftharpoons S$
HP_2	$Liquid_{HP_2} + X \rightleftharpoons T$
IE_2	$Liquid_{IE_2} \rightleftharpoons T + \beta$

The eutectic curve E_1P_1 has a maximum point and it proceeds from this point to both E_1 and P_1 points.

Table 4.

Invariant Points	Composition			Temperature °C	Reaction
	Cu %	Mg %	Al %		
E1	26.8	6.2	Rest	500	$Liquid \rightleftharpoons (Al)_k + CuAl2 + S$
E2	3	32	,,	447	$Liquid \rightleftharpoons (Al)_o + T + \beta$
P1	11	25	,,	465	$Liquid + S \rightleftharpoons T + (Al)_k$
P2	14	29.5	,,	525	$Liquid + X \rightleftharpoons T + S$

It will clearly be seen in this investigation that there exist four invariant points on the liquidus surface, whose composition and reacting phases are given in Table 4.

The solidus surface of (Al)-solid solution exists in the domain Aakmop, and its solubility decreases to Aclnpo, at room temperature. On this solid solubility surface there exist the solid reaction lines

kl $(Al) \rightleftharpoons CuAl_2 + S$
mn $(Al) \rightleftharpoons S + T$
op $(Al) \rightleftharpoons T + S$

Summary.

In conclusion, the present investigations are summarized as follows:

(1) The Equilibrium Diagram of Al-rich Al-Cu-Mg alloys was determined.

(2) Two ternary compounds to be in equilibrium with Al-solid solution were found to exist in this diagram. They correspond to $Al_{13}Cu_7Mg_8$ and Al_5CuMg_4 respectively and they are called S and T.

(3) In the domain of the present investigation the following uni-variant lines were found to exist

$Liquid \rightleftharpoons (Al) + CuAl_2$
$Liquid \rightleftharpoons (Al) + S$
$Liquid \rightleftharpoons (Al) + T$
$Liquid \rightleftharpoons (Al) + \beta$
$Liquid \rightleftharpoons CuAl_2 + S$
$Liquid + T \rightleftharpoons S$
$Liquid + X \rightleftharpoons S$
$Liquid + X \rightleftharpoons T$
$Liquid \rightleftharpoons T + \beta$,

and as invariant reactions,

$Liquid \rightleftharpoons (Al) + CuAl_2 + S$
$Liquid \rightleftharpoons (Al) + T + \beta$
$Liquid + S \rightleftharpoons T + (Al)$
$Liquid + X \rightleftharpoons T + S$

were observed.

(4) The solid reaction lines

$(Al) \rightleftharpoons CuAl_2 + S$
$(Al) \rightleftharpoons S + T$
$(Al) \rightleftharpoons T + \beta$

were observed to exist in (Al) solid solution.

Acknowledgment.

In conclusion, the writer would like to express his cordial thanks to Doctor H. Hisatsune, Mr. M. Shobu, and others who gave much assistance in this research. The writer's thanks are also due to the Hattori-Hoko-Kwai, a subsidy from which enabled his research to be undertaken.